

S

Cell



the association between the consumption of sugar-sweetened food and pancreatic cancer risk ([Larsson et al., 2006](#)). Even with the strong association observed between diabetes and pancreatic cancer, causality remains problematic. If T2D were directly driving pancreatic cancer risk, it would be expected that the increased duration of diabetes diagnosis would be associated with the ever-increasing risk of pancreatic cancer. By contrast, the epidemiological data indicate that the highest risk of pancreatic cancer is observed soon after T2D diagnosis, with the risk decreasing over time ([Bosetti et al., 2014](#)), a kinetic that suggests that at least part of the risk is driven by undiagnosed pancreatic cancer causing T2D. In addition to this, the known association of T2D with obesity and altered diet increases the potential for confounding associations ([Gumbs, 2008](#); [Hart et al., 2008](#)). To the extent possible, these confounding factors are controlled for; however, there is a limit to the accuracy that can be achieved in monitoring food intake. These limitations are of particular importance in case-control studies of pancreatic cancer, in which the long latency period and strong impact on appetite can reverse causality ([Sanchez et al., 2012](#)).

The epidemiological associations of pancreatic cancer with diet, obesity, and T2D are extremely complex to unravel. It is therefore difficult, using human studies alone to determine whether diet, obesity, and T2D independently contribute to the risk of pancreatic cancer development or whether some or all

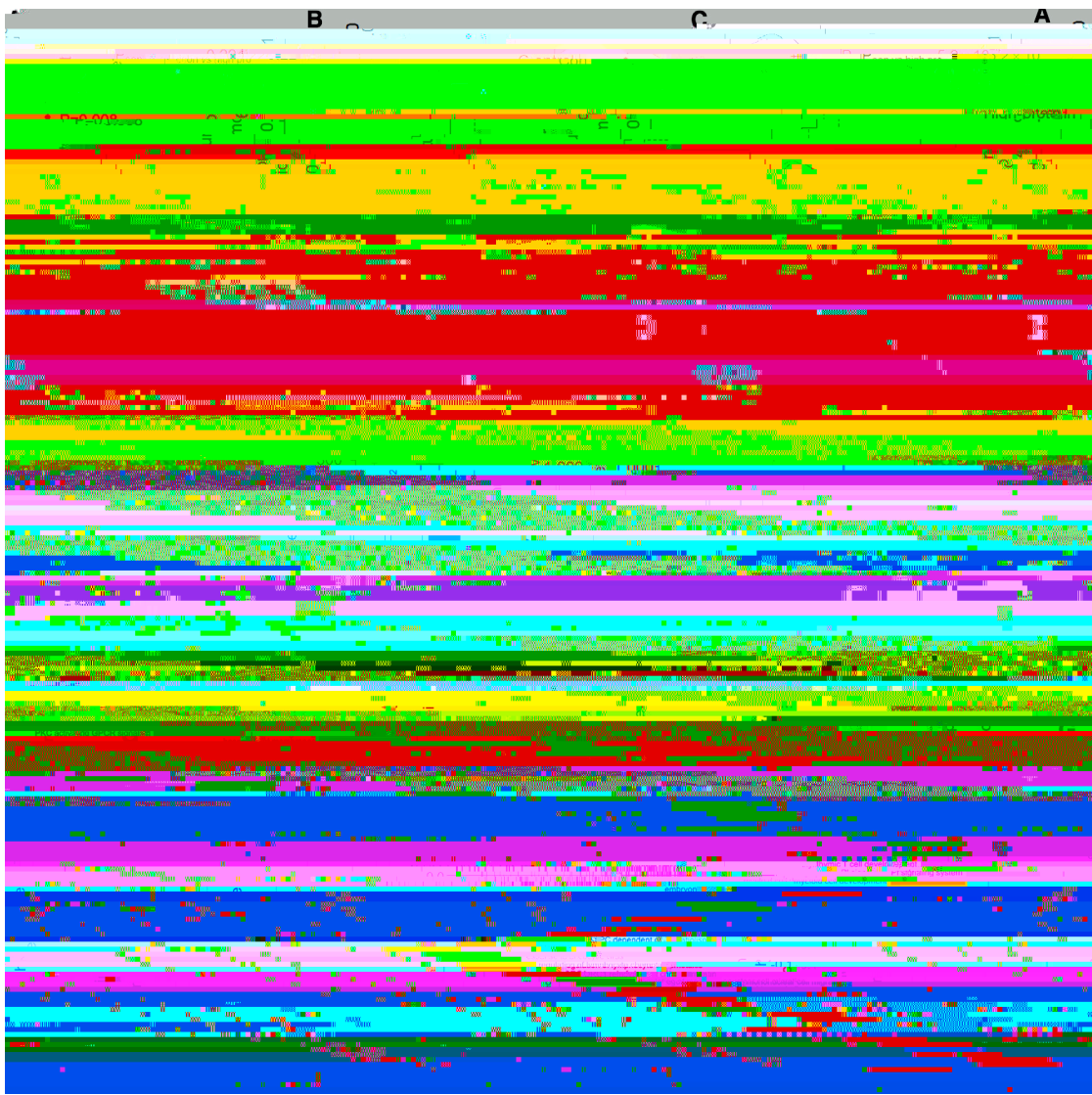


Figure 2. High-Protein Diet Inhibits Pancreatic Cancer Onset and Reduces the Expression of Cell-Cycle Components

TAg⁺ mice were placed on either a control or a high-protein diet and assessed through MRI.

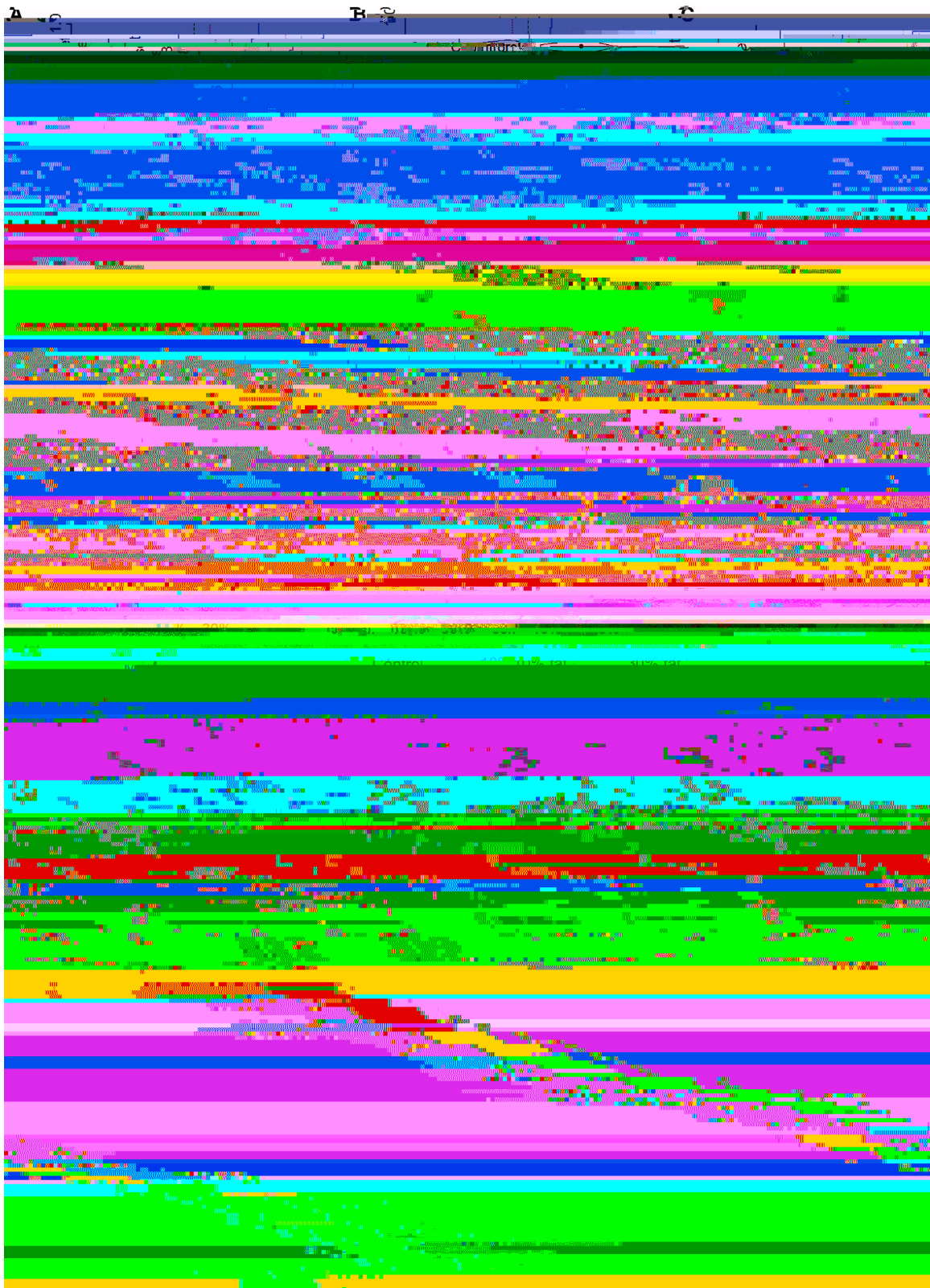
(A and B) Cumulative incidence of pancreatic cancer in mice on a control diet ($n = 17$) or a high-protein diet ($n = 6$) for female mice (A), or a control diet ($n = 19$) or a high-protein diet ($n = 4$) for male mice (B). p values via log-rank test.

(C) Age at tumor onset. p values via Mann-Whitney test.

(D) Tumor volume increase every 2 weeks. p values via Mann-Whitney test.

composition of the sugar-free diet (see below), demonstrating the complexity of a multifactorial nutritional analysis. Analysis of tumor growth rates found a trend toward higher sugar levels' driving more rapid tumor expansion (Figure 4D). At the histological level, a clear dose-dependent effect of the glucose content of the diet on tumor cell proliferation and density was observed (Figures 4E–4G). A large effect of sugar was also observed on

tumor-induced mortality, with high-glucose diets driving early-onset mortality (Figures 4H and 4I), and the sugar-free diet significantly delaying mortality in female mice (Figure 4I). At a transcriptional level, the tumors from high-glucose-fed mice exhibited an elevated expression of cell-cycle genes and ribosome components compared to sugar-free-fed mice (Figures 4J and S5). Metabolic profiling revealed a reduction in amino acid levels



(legend on next page)

in the tumors from high-glucose-fed mice (Figure 4K), possibly indicating that amino acids were actively used for protein synthesis. We then tested the association between blood glucose level and upregulation of the cell-cycle signature within the tumor. Across the range of diets used in this study, mice with higher blood glucose levels showed a tendency toward high expression of the cell-cycle signature (Figure 4L). These data indicate that dietary sugar (or downstream mediators, such as insulin) enhances the cell cycle and upregulates the ribosomal capacity,

more similar regardless of the diet ([Figures 6D](#) and [6E](#)). This

strongly associated with pancreatic cancer ([Mayers et al., 2014](#)). A potential unification of these discrepancies may lie in the origin of these BCAAs, with pancreatic cancer associated with the

caution that even dietary interventions that succeeded in slowing tumor growth may not affect mortality.

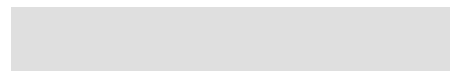
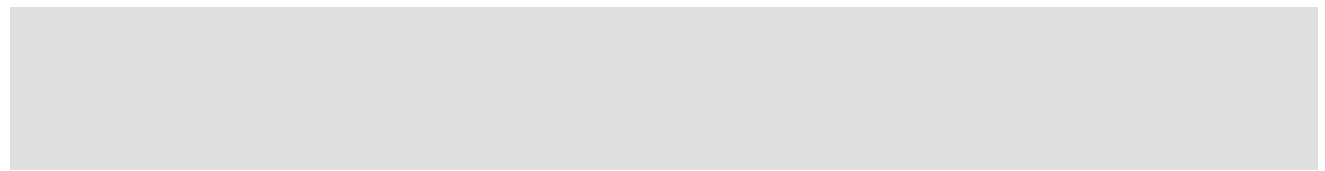
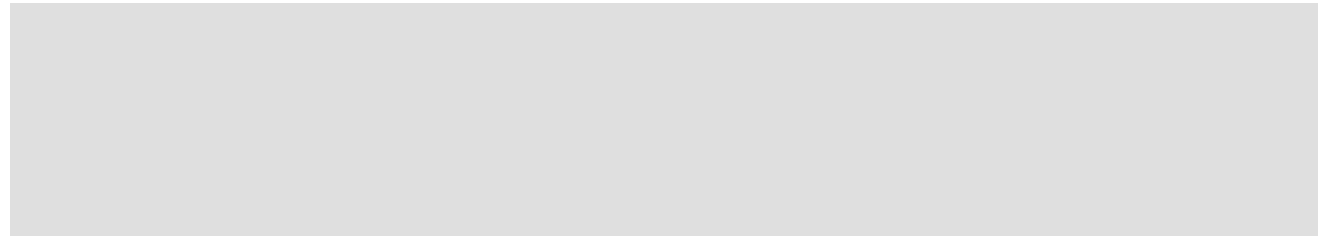
STAR +METHODS

Danai, L.V., Babic, A., Rosenthal, M.H., Dennstedt, E.A., Muir, A., Lien, E.C.,
Mayers, J.R., Tai, K., Lau, A.N., Jones-Sali, P., et al. (2018). Altered exocrine

- Saloman, J.L., Albers, K.M., Cruz-Monserrate, Z., Davis, B.M., Edderkaoui, M., Eibl, G., Epouhe, A.Y., Gedeon, J.Y., Gorelick, F.S., Grippo, P.J., et al. (2019). Animal Models: Challenges and Opportunities to Determine Optimal Experimental Models of Pancreatitis and Pancreatic Cancer. *Pancreas* 48, 759–779.
- Sanchez, G.V., Weinstein, S.J., and Stolzenberg-Solomon, R.Z. (2012). Is dietary fat, vitamin D, or folate associated with pancreatic cancer? *Mol. Carcinog.* 51, 119–127.
- Scintu, M., Vitale, R., Prencipe, M., Gallo, A.P., Bonghi, L., Valori, V.M., Maiello, E., Rinaldi, M., Signori, E., Rabitti, C., et al. (2007). Genomic instability and increased expression of BUB1B and MAD2L1 genes in ductal breast carcinoma. *Cancer Lett.* 254, 298–307.
- Scott, R.A., Freitag, D.F., Li, L., Chu, A.Y., Surendran, P., Young, R., Grarup, N., Stancaková, A., Chen, Y., Varga, T.V., et al.; CVD50 Consortium; GERA-D_EC Consortium; Neurology Working Group of the Cohorts for Heart; Aging Research in Genomic Epidemiology (CHARGE); Alzheimer's Disease Genetics Consortium; Pancreatic Cancer Cohort Consortium; European Prospective Investigation into Cancer and Nutrition–Cardiovascular Disease (EPIC-CVD); EPIC-InterAct; CHARGE Consortium; CHD Exome+ Consortium; CARDIOGRAM Exome Consortium (2016). A genomic approach to therapeutic target validation identifies a glucose-lowering GLP1R variant protective for coronary heart disease. *Sci. Transl. Med.* 8, 341ra76.
- Siegel, R.L., Miller, K.D., and Jemal, A. (2016). Cancer statistics, 2016. *CA Cancer J. Clin.* 66, 7–30.
- Sievert, C. (2020). Interactive Web-Based Data Visualization with R, *plotly*, and *shiny* (CRC Press).
- Smith, C.A., Want, E.J., O'Maille, G., Abagyan, R., and Siuzdak, G. (2006). XCMS: processing mass spectrometry data for metabolite profiling using nonlinear peak alignment, matching, and identification. *Anal. Chem.* 78, 779–787.
- Tevethia, M.J., Bonneau, R.H., Griffith, J.W., and Mylin, L. (1997). A simian virus 40 large T-antigen segment containing amino acids 1 to 127 and expressed under the control of the rat elastase-1 promoter produces pancreatic acinar carcinomas in transgenic mice. *J. Virol.* 71, 8157–8166.
- Therneau, T.M., and Grambsch, P.M. (2000). *Modeling Survival Data: Extending the Cox Model* (Springer).
- Vander Heiden, M.G., Cantley, L.C., and Thompson, C.B. (2009). Understanding the Warburg effect: the metabolic requirements of cell proliferation. *Sci.*

STAR + METHODS

KEY RESOURCES TABLE



RESOURCE AVAILABILITY

Lead Contact

tallow-derived; 17.8% w/v sugar, 30.1% w/v fat, 20.8% w/v protein), high glucose diet (ssniff® EF R/M High glucose; 50.0% w/v sugar, 2.9% w/v fat, 19.1% w/v protein) and sugar-free diet (ssniff® EF R/M Glucose free, low CH; 2.0% w/v, 11.3% w/v fat, 52.5% w/v protein). Where indicated, drinking water was modified through the addition of 5% w/v glucose, 5% w/v fructose or 5% w/v sucrose. Except where indicated ("switched"), all dietary exposures were continual from the in utero stage onward, with breeder cages set up on the indicated diet, and transfer of pups at weaning to the same dietary exposure. Average daily food intake for the different diets was measured in a parallel wild-type cohort ([Figure S4A](#)), however individual variation in the total food intake of tumor mice was not measured. Mice were bred under specific pathogen-free conditions and moved to conventional conditions at seven weeks of age for longitudinal magnetic resonance imaging (MRI). Mouse housing conditions were kept at 20°C. All mice were used in accordance with the University of Leuven Animal Ethics Committee. Mouse-weight and non-fasting blood glucose were monitored throughout, in the mid-afternoon.

Human subjects

For evaluating the effect of diet on pancreatic cancer, we included individuals from the European Prospective Investigation into Cancer and Nutrition (EPIC) cohort with collected epidemiological information at the time of recruitment (1992-2000) for medical history, anthropometric measures and lifestyle/dietary characteristics. Personal identifying information, as available at local centers, is not transferred to the Internal Review Board of the International Agency for Research on Cancer (IARC) co-ordinating center. Informed consent was provided by each participant, and projects using the EPIC resource need to be cleared by both the IARC and local ethical review committees. For this analysis, epidemiologic and dietary data was available for 459,231 individuals [1,314 pancreatic cancer cases (males = 561 with $\text{age}_{\text{recruitment}} = 57.07 \pm 7.35$ (mean \pm SD) and $\text{age}_{\text{exit}} = 66.45 \pm 8.29$; females = 753 with $\text{age}_{\text{recruitment}} = 57.36 \pm 7.66$ and $\text{age}_{\text{exit}} = 7.012$] TJ/F171Tf3.456830TD(HTj/F41Tf.84350TD((7.5(3))-235.8(agd)-242(a457,917-236.23non-fases)-204.2(o(males)-135.81)-139.85(33.539-204.with)-2340age

A21472) and DAPI (Life Technologies, D1306). Images were acquired using a Zeiss 780 confocal microscope. Images were analyzed using ImageJ (National Institute of Health, Bethesda, USA) to calculate MFI on a per cell basis utilizing watershed function and

Nutritional landscape analysis was performed using “vegan” package in R, a two-dimensional coordination of all groups was first constructed based on the diet compositions (based on weight/volume of each macronutrient and overall energy density) using principle component analysis (PCA), and each nutrient component or mouse phenotype can be then plotted according to their averaged

the departure from the multiplicative effects of the corresponding main effects and can be interpreted as the increase in pancreatic cancer risk with one gram per day increase in the nutrient. The GxE interaction tests were conducted using the freely available software QUICKTEST v0.95 ([Kutalik et al., 2011](#)).

Untargeted metabolomics analysis

For untargeted metabolomics, peaks were extracted using XCMS ([Smith et al., 2006](#)